PHYSICSAccess Research Paper
ISSN Online: 2756-3898, ISSN Print: 2714-500X https://doi.org/10.47514/phyaccess.2025.5.1.004

Delineation of Groundwater Aquifer and Subsurface Structures of Some Selected Areas in Chikun Local Government Area of Kaduna State, Nigeria using Electrical Resistivity

Adeka Patience[1], Cyril G Afuwai[1], Matoh D Dogara[1], Garba M Ephraim[2], Magaji Simon[3] and Ezra Dauda[1]

[1] Department of Physics, Kaduna State University, Kaduna State, Nigeria
[2] Department of Physics, Kaduna state college of Education Gidan Waya, Kaduna State, Nigeria
[3] Department of Physics, Kaduna State College of Nursing Kafanchan, Kaduna State, Nigeria

Corresponding E-mail: pacyadeka@gmail.com

Received 16-11-2024
Accepted for publication 27-01-2025
Published 07-02-2025

Abstract

This study is aimed at delineating groundwater aquifer and subsurface structures of some selected areas within Chikun local government area of Kaduna State, Nigeria, using the Vertical Electrical Sounding (VES) method. To obtain the electrical resistivity values of the subsurface within the study area, electric current was conducted into the ground through two current electrodes while measuring the corresponding values of the potential difference using two potential electrodes. VES was conducted in twenty (20) different stations and was named profiles A, B, C and D with each having five stations with several layers, and four Vertical Electrical Sounding curves which were A, H, Q and QH were obtained. The results obtained from Vertical Electrical Sounding (VES) revealed the aquifer was at depths 7.3 m, 0.141 m 22.7 m, and 14 m for VES A, B, C and D respectively. Results from the 2D map revealed low resistivity within the weathered basement and fracture basement with resistivity values ranging between 1.929 – 885 Ωm which correlates with the results obtained from the VES. The reflection coefficient (r) was used to determine the aquifer protective capacity of the study area and the isoresistvity map depicted that 7% was good (with r values ranging between 0.8 – 4.9), 43% was moderate (with r values ranging between 0.2 - 0.79), 33% was weak (with r values ranging between 0.10 - 0.19) and 17% was poor (with r values <0.10). Aquifer with low reflection coefficient values ($r<0.8$) favors groundwater potentiality but with high vulnerability to contamination. The study area has an aquiferous zone characterized by fractures and porosity aiding groundwater permeability and storage.

Keywords: Delineation; VES; Aquifer; Subsurface; Resistivity.

I. INTRODUCTION

Delineation of groundwater aquifer and subsurface structures is simply a way of identifying and mapping areas or boundaries portraying characteristics that signifies the presence of underground water-bearing formations [1]. To achieve this, geophysical methods such as electrical resistivity, gravity surveys, magnetic surveys, and sometimes ground penetrating radar (GPR) are employed [2]. These aquifers are simply underground layers of rocks and sediments that contain water which serves as an important source of fresh drinking water and farming purposes [3]. Delineating aquiferous zones is essential due to the high demand for freshwater arising from the increase in world population. As the population of any area increases, so also does the demand for freshwater increase in equal proportions because water is required for different purposes such as drinking, bathing, industrialization, farming, etc.. [4]. The rapid increase in population is associated with urbanization and economic development, which affect the level of water usage per capita both in terms of actual water use as well as the virtual water content of products consumed [5]. To match the increase in population, irrigation farming is practiced due to the increase in food demands which require water. The practice of irrigation farming has now become a global venture and is aimed at meeting the world's needs. This expansion of irrigated agriculture, especially in semiarid areas with limited precipitation and surface water has eventually raised the global need for reliance on irrigated crops on groundwater withdrawal [3]. These activities such as irrigated farming and industrialization do cause challenges on the access to clean surface water thereby making the delineation of water-bearing formation in urban areas necessary [6]. Consequently, the steady increase in the use of non-renewable groundwater is taken out of the aquifers that will likely not be replenished on human time scales [7]. This scenario occurs in virtually all urban areas such as Chikun local government area of Kaduna State, Nigeria because of human activities associated with the growing population and industrialization. Chikun is one of the 23 local government areas of Kaduna state and is one of those local governments that form Kaduna central and is densely populated due to social institutions situated within it and, insecurity has forced people to desert villages and eventually settle in some parts of Chikun local government. To curtail the challenges of getting fresh clean water to match the growing population of the area, a study to delineate groundwater aquifer and subsurface structures is crucial. A study on delineating groundwater aquifer and subsurface structures is usually conducted using different geophysical methods such as geo-electrical, electromagnetic, ground penetrating radar (GPR), gravity, magnetic and seismic to delineate subsurface architecture and mineral exploration. Several research [2, 3, 5, 7] revealed that groundwater usually has some dissolved electrolytes, and the mobility of its ions makes it conductive, thereby allowing electric current to flow through them. Reference [8] used electrical resistivity methods to image the Earth by measuring the potential generated by injecting direct current (DC) into the ground. The information received were geoelectrical images that displayed the spatial distribution of resistivity which could be related to different types of soil and rock.

Also, in the quest to delineate water-bearing formations (aquiferous zones), [9, 10] used the theory and application of the electrical resistivity method for groundwater investigations.

The electrical resistivity technique has the following advantages: (i) it can be applied to any field with ease (ii) it can reveal information on depths ranging from a few meters to hundreds of meters beneath the surface, and (iii) the availability of software for 2D and 3D interpretation. It can be used to solve many hydro-geological challenges such as monitoring industrial waste contamination, determination of the spatial extent of groundwater aquifers [11] and studying and monitoring aquifer recharge ponds [12].

In this study, electrical resistivity was used to Delineate Groundwater Aquifer and Subsurface Structures of Some Selected Areas in Chikun Local Government Area of Kaduna State, Nigeria.

II. MATERIALS AND METHOD

A. Location and Geology of the Study Area

1) Location

Chikun LGA is one of the 23 LGAs of Kaduna State. Kaduna State is one of the thirty-six states of the Federal Republic of Nigeria, Chikun lies between Latitude 100 25′ 31″ N and10037′ 38″and Longitude 70 01′ 09″ E and 70 29′ 50″ E. Chikun LGA has an area of 4,645 km² and mean elevation of 620 m above mean sea level, Ungwan Maigero and Narayi are towns within Chikun L.G.A. The local government have a population of about 502,500 people [12]. The map of the study area is shown in Fig. 1.

2) Geology of the Area

This study is situated within Nigeria's Crystalline Basement Complex, the area lies between the Guinea savannah belts, with two tropical climates with two distinct seasons: the rainy season which begins around April and ends in October and the dry season running from November through March. The average annual rainfall in Kaduna is 300 mm. Rainfall generally reaches its peak in August and its mean temperature of about 29 ^{0}C in March/April. The major River Kaduna controls the course of most of the rivers [13]. The sites are accessible on foot, bicycle and motorcycle.

B. Materials

The materials used in the research paper include Oasis Montaj software, Ohmega resistivity meter, Measuring tape, Current wires, Electrodes, Res 1d version 1.00.07 beta modelling software, Hammer, Connecting wires, and Global positioning system (GPS).

C. Method

1) Data Collection

Water hydrochemistry of thirty (30) water samples from boreholes was taken from various locations and listed as depidted in Tables I and II. All the boreholes in the study area were functional except those of Engr Dele Street, D Ziggau Street, Okeymax Avenue, Mission Street, Riverside and Rhema church. In the comparison of data from these boreholes, patterns in the geological formations were recognized allowing delineation of the aquiferous zone because borehole data such as water level and hydraulic conductivity are crucial in assessing the aquiferous zone and its conductivity. Therefore, these non-functional boreholes could be due to the failure to reach the water-bearing formation (aquiferous zone) during the borehole drilling.

Five vertical electrical soundings $(A_1, A_2, A_3, A_4, A_5)$ points were evenly distributed across selected points within the study area and the Schlumberger array configuration was to collect data. The Wenner array configuration was used for 2-D imaging since it is moderately sensitive to horizontal and vertical geological structures. The two techniques were used because they will aid in understanding the lithology and groundwater exploration of the study area. Eight 2-D stations were carried out and the electrodes were arranged at an equidistance of $10\,m$ during data collection. To obtain the electrical resistivity values of the subsurface within the study area, an electrical current was led in the ground through current electrodes and the voltages were measured using the potential electrodes; the geological characteristics of the Earth's subsurface were inferred from these properties. The global positioning system was used to determine the longitudes, latitudes, and elevations of various sites of interest [14].

Table I. Borehole status report of the study area.

S/N	Longitude	Latitude	Elevation	Borehole status	Borehole location
1.	N 10^0 29.048	E 007^0 26.817	581 m	Functional	Bishop Kukah's Close
2.	N 10^0 29.103	E 007^0 26.837	580 m	Functional	Abia Street Learner's Junction
3.	N 10^0 29.048	E 007^0 26.071	590 m	Functional	Engr. Gana Street
4.	N 10^0 29.104	E 007^0 27.051	595 m	Non-Functional	Engr. Dele Street
5.	N 10^0 29.125	E 007^0 27.078	593 m	Functional	Engr. Gana Close
6.	N 10^0 29.191	E 007^0 27.075	596 m	Functional	Church Road Maigero
7.	N 10^0 29.221	E 007^0 27.136	596 m	Functional	Pius Musa Close
8.	N 10^0 29.216	E 007^0 27.171	594 m	Non-Functional	D Ziggau Street
9.	N 10^0 29.187	E 007^0 27.051	595 m	Functional	Fedelis D thot Street
10.	N 10^0 29.175	E 007^0 27.279	594 m	Functional	Adisman Kolawole Street
11.	N 10^0 29.084	E 007^0 27.254	591 m	Non-Functional	Okeymax Avenue
12.	N 10^0 29.044	E 007^0 27.242	592 m	Functional	Sarki Street
13.	N 10^0 29.068	E 007^0 27.292	598 m	Functional	Learners Street
14.	N 10^0 29.067	E 007^0 27.422	598 m	Functional	Water intake Maigero
15.	N 10^0 29.048	E 007^0 29.480	603 m	Non-Functional	Mission Street
16.	N 10^0 29.073	E 007^0 27.496	602 m	Functional	JJ Closed by NNPC Water intake
17.	N 10^0 29.066	E 007^0 27.522	603 m	Functional	Ekeoma Drive
18.	N 10^0 29.023	E 007^0 27.529	603 m	Functional	Joseph Sule Close
19.	N 10^0 29.970	E 007^0 27.648	604 m	Functional	Little Lamb Drive
20.	N 10^0 29.086	E 007^0 27.650	609 m	Functional	Horns of Salvation Avenue

Table II. Borehole survey report for the study area.

S/N	Longitude	Latitude	Elevation	Borehole status	Borehole Location
1.	N 10^0 29.017	E 007^0 26.635	610 m	Functional	Fedeco Road
2.	N 10^0 28.877	E 007^0 26.681	587 m	Functional	Buruku Road
3.	N 10^0 28.798	E 007^0 26.766	579 m	Functional	Kano Road
4.	N 10^0 28.675	E 007^0 26.295	597 m	Functional	Zaria Road
5.	N 10^0 29.074	E 007^0 26.590	589 m	Non-Functional	Rhema Church
6.	N 10^0 29.074	E 007^0 26.563	591 m	Functional	Narayi Road
7.	N 10^0 29.104	E 007^0 26.565	580 m	Non-Functional	Riverside
8.	N 10^0 29.070	E 007^0 26.682	586 m	Functional	Aliyu Makama Close
9.	N 10^0 29.003	E 007^0 26.74	584 m	Functional	Fedeco close
10.	N 10^0 28.617	E 007^0 26.852	599 m	Functional	Dokaje Street

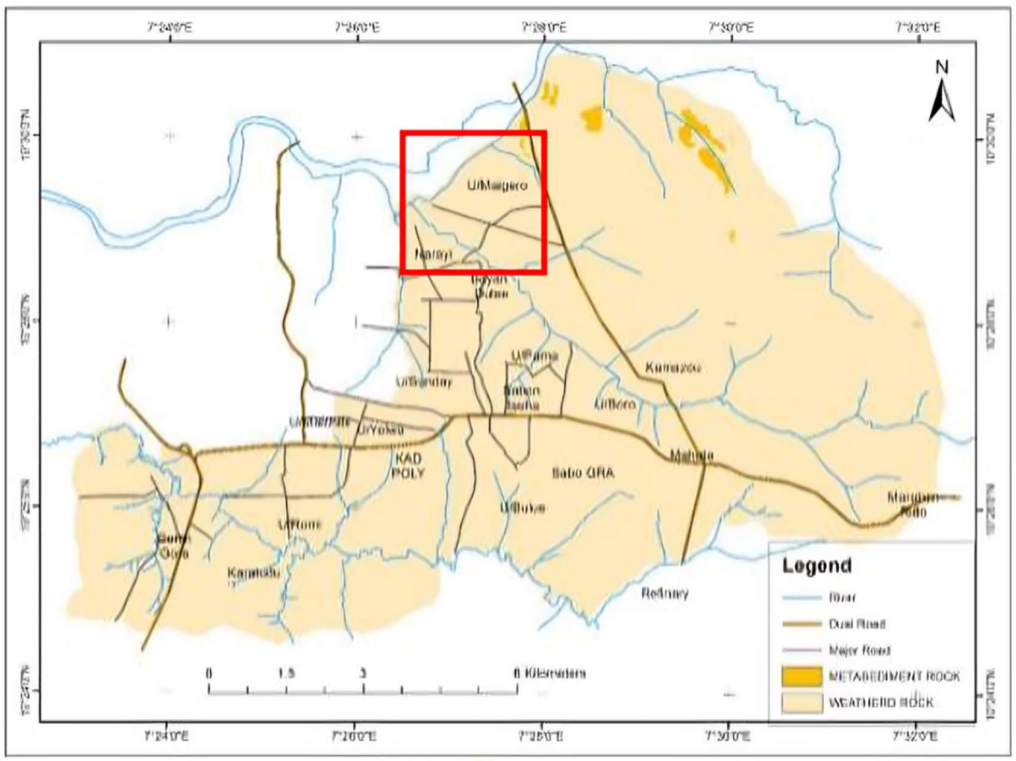

Fig. 1. Map of the study area.

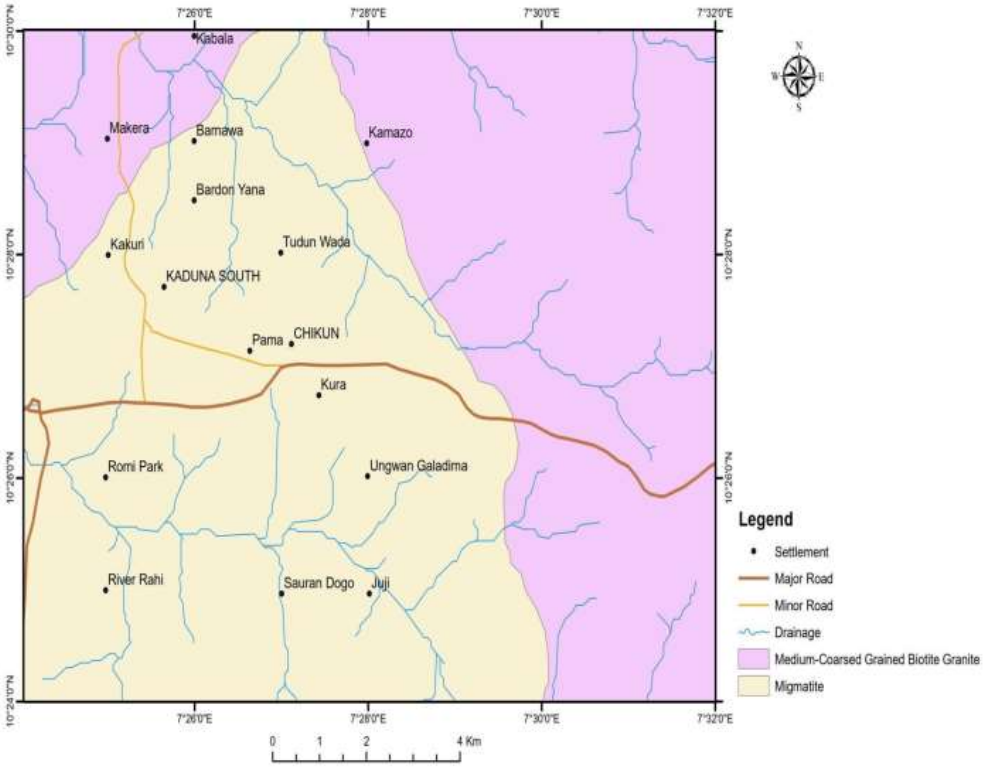

Fig. 2. Geological map of Chikun.

2) Data acquisition

Data acquisition was achieved using a Wenner configuration in which the electrodes were arranged with equal spacing "a" equals $C_1P_1 = P_1P_2 = P_2C_2$, where C_1, C_2 *and* P_1P_2 are the current and potential electrodes 1 and 2 respectively. This arrangement entails moving the array over a traverse line, while horizontal variations can alternatively be explored using individual measurements taken at grid points [15]. A 2-dimensional design was used for the field acquisition design as presented in Fig. 4.

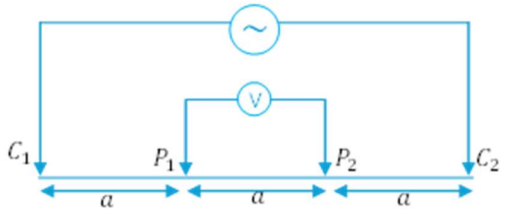

Fig. 3. Wenner Configuration.

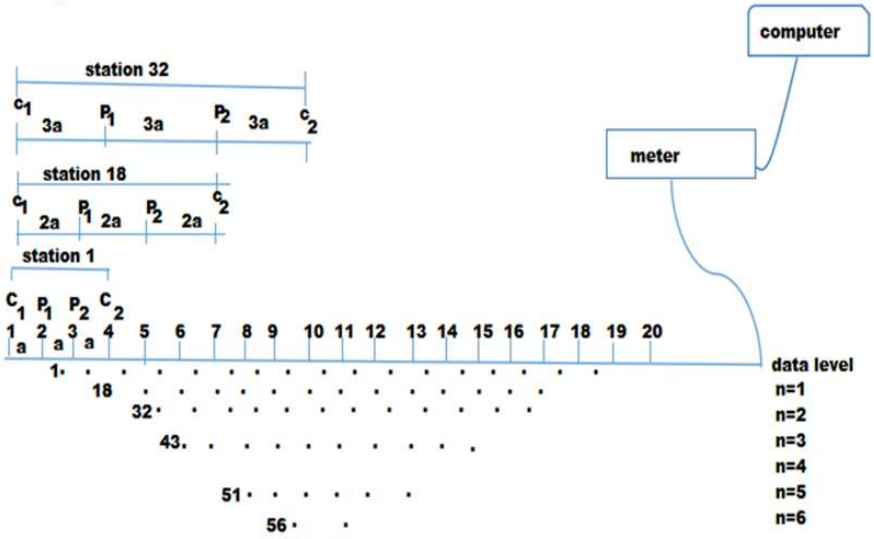

Fig. 4. 2D Survey Design with Wenner Configuration.

During data acquisition, the potential difference value (ΔV) produced an amount of current (I) such that the resistivity ρ can be calculated using (1):

$$\rho = k\frac{\Delta V}{I} \quad (1)$$

Where k is a geometry factor, which is expressed by (2).

$$K = 2\pi a \quad (2)$$

However, current I and potential V in a metal conductor at constant temperature are connected as in (3) according to Ohm's law:

$$V = IR \quad (3)$$

Where R, the proportionality constant is the resistance, measured in ohms (Ω). A conductor's resistance R is proportional to its length L and cross-sectional area A as given in (4).

$$R = \frac{\rho L}{A} \quad (4)$$

Where the resistivity is a property of the material under consideration.

During the field procedure, the following precautions were taken.

a) It was ensured that the electrodes penetrated well into the ground to have good contact by hammering it deep into the ground.
b) It was ensured the connection was carefully made.
c) Caution was taken while laying the wires for effective current flow.
d) The resistivity meter was turned off after each successive reading and ON when taking the next reading.

During the 2D survey design, the Wenner configuration started by positioning the electrodes C_1, P_1, P_2, C_2 corresponding to positions 1, 2, 3 and 4 for the first measurement. The arrangement of electrodes was shifted sequentially such that the second measurement would have electrodes positioned 2, 3, 4 and 5, and the third measurement with electrodes positioned 3, 4, 5 and 6. The measurement continued with the same pattern of shifting the electrodes while maintaining equidistance until the end of the entire landscape. To Process and analyse the resistivity data, the RES2DINV program was used. This program operates effectively because the inversion of quasi-Newton is embedded in the software and makes the analytical calculation of the Jacobian matrix for a homogeneous half-space for the first iteration possible. Also, it helps to interpret the Vertical Electrical Sounding (VES) data for Schlumberger, Wenner, and other arrays [13] and to determine the vertical variation in resistivity as a function of depth [14]. This feat is predicated on the assumption that the surface is homogeneous and isotropic [16].

3) Vertical Electrical Sounding (VES)

Potential electrodes MN are inserted between current electrodes AB in the Schlumberger design, with a central reference point formed. At each reading, the current electrodes AB are symmetrically pushed outward for deeper current penetration and probing. When the current electrodes AB are relatively far apart, the distance between the MN electrodes is increased but MN remains much less than AB [1]. This is done to ensure quantifiable potential and to keep the voltage from falling below the voltmeter's reading accuracy. When the current electrode is placed on the surface of the equipotential surface and is semi-spherical downward into the ground, a potential gradient is observed at M and N. The surface area of the sphere will thus be $2\pi r^2$, where r is the radius. Thus,

$$V = \frac{\rho I}{2\pi r^2} \quad (5)$$

Then, the potential at M which is V_M, due to the two current electrodes, is

$$V_M = \frac{I\rho}{2\pi}\left(\frac{1}{r_1} - \frac{1}{r_2}\right) \quad (6)$$

Similarly, the potential at electrode N which is V_N is given by

$$V_N = \frac{I\rho}{2\pi}\left(\frac{1}{r_3} - \frac{1}{r_4}\right) \quad (7)$$

Where r_1, r_2, r_3 and $r_4$separations as shown in Fig. 5.

The potential difference, ΔV, existing across electrodes M and N is given by.

$$\Delta V = V_M - V_N = \frac{I\rho}{2\pi}\left[\left(\frac{1}{r_1} - \frac{1}{r_2}\right) - \left(\frac{1}{r_3} - \frac{1}{r_4}\right)\right] \quad (8)$$

$$\Rightarrow \frac{2\pi\Delta v}{I}\left[\frac{1}{\left(\frac{1}{r_1} - \frac{1}{r_2}\right) - \left(\frac{1}{r_3} - \frac{1}{r_4}\right)}\right. = \rho \quad (9)$$

Given that practically the body is inhomogeneous, apparent resistivity (ρ_a) is considered,

$$\rho_a = \frac{K\Delta V}{I} \quad (10)$$

Where ρ_a apparent resistivity in Ωm and K is called the geometric factor whose value depends on the type of electrode array used.

$$2\pi\left[\frac{1}{\left(\frac{1}{r_1} - \frac{1}{r_2}\right) - \left(\frac{1}{r_3} - \frac{1}{r_4}\right)}\right. = K \quad (11)$$

For Schlumberger configuration, if $MN = 2b$ and $r = \frac{AB}{2}$, then,

$$K = \pi\left(\frac{r^2}{2b} - \frac{b}{2}\right) \quad (12)$$

1) Reflection coefficient (r)

The reflection coefficient r is given by (13).

$$\mathrm{r} = \frac{[(\rho^{\mathrm{n}} - \rho(\mathrm{n}-1)]}{[(\rho^{\mathrm{n}} + \rho(\mathrm{n}-1)]} \quad (13)$$

Here ρ^{n} represents resistivity of the nth layer, ρ(n−1) is the layer resistivity overlying the nth layer. This mathematical equation is embedded in software such as MATLAB and Oasis Montaj for easy computation. If the value in (13) is low, it implies a fractured or weathered bedrock associated with groundwater potential. However, if the r value is greater than 0.8, then it is considered very favorable to aquifer protection [18].

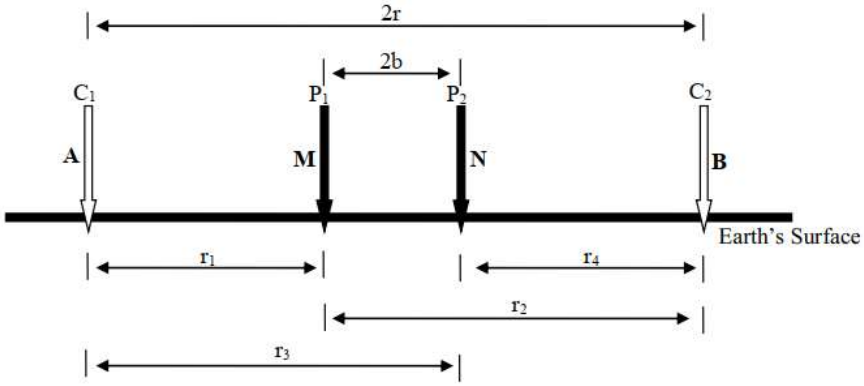

Fig. 5. Schlumberger Electrode Array.

III. RESULTS AND DISCUSSION

The results obtained through VES (using Wenner array) of the 20 stations are presented in Tables III, IV, V and VI of which profiles A, B, C and D represent five stations in each case. However, the resistivity values and thickness of each layer obtained across the study area were given and written in terms of the curve types [17]. The type of curves identified from the VES of profile A (see Table III) were all H- curve ($\rho_1 > \rho_2 < \rho_3$), VES of profile B (see Table IV) were all A-curve ($\rho_1 < \rho_2 < \rho_3$) except B_1 which was H-curve, VES of profile C (see Table V) were of H-curve except C_3 which was A-curve and the VES of profile D (see Table VI) had an H-curve type in ($D_1 - D_3$) while D_4 and D_5 had QH- curve ($\rho_1 > \rho_2 > \rho_3 < \rho_4$) and Q-curve ($\rho_1 > \rho_2 > \rho_3$) respectively. Dar Zarrouk parameters were obtained, and field data such as coordinates and elevations of all the chosen points were all used to produce a curve-types; and maps of various geoelectric sections (based on aquifer pattern and bedrock characterization)of the study area (Fig. 5 – 8). The geoelectric sections of the study area were done to visualize the vertical and lateral distributions of the apparent resistivity layer-by-layer in the subsurface which revealed lateral and vertical face changes inferred from the geoelectrical parameters [17]. From

the geoelectrical sequences, inferred geoelectric layers were topsoil, weathered basement, fresh basement and fracture basement.

A. Iteration Result and Lithology of the Study Area

Table III is a result of profile A showing vertical electrical sounding (VES) curves along it with three (3) stratigraphic units interpreted as Topsoil, weathered basement and fresh basement. All the VES were of the H-curve ($\rho_1 > \rho_2 < \rho_3$) type. The topsoil and weathered basement had resistivity and thickness ranges of $66.061 - 299.733\ \Omega m, 0.7 - 2.84\ m$ and $24.269 - 86.319\ \Omega m, 4.48 - 12.7\ m$ respectively while the fresh basement resistivity range $1445.5 - 3403.481\ \Omega m$, showing the highest aquifer potential is found in areas with a thickness of $12.7\ m$ while the least aquifer potential was in areas with a thickness of $4.48\ m$.

Table IV is profile B's geoelectric and geologic section with three interpreted layers: Topsoil, weathered basement, and fresh basement. All the curve types as shown in Table IV are A's types ($\rho_1 < \rho_2 < \rho_3$) except B1 having H-types ($\rho_1 > \rho_2 < \rho_3$). The topsoil resistivity ranges from $25.5 - 1329\ \Omega m$ and thickness ranging from $0.141 - 4.32\ m$. The weathered basement has resistivity ranging from $156 - 1150\ \Omega m$ and a thickness ranging from $7.652 - 65.359\ m$. The fresh basement has resistivity ranging from $2328.0 - 3448.5\ \Omega m$.

Table III. Result and Lithology of Geoelectrical section of profile A.

S/N	Layers	Resistivity (Ωm)	Thickness (m)	Depth (m)	Curve Type	Probable Lithology
A_1	I	215.387	2.844	2.844	H	Topsoil
	II	34.463	4.48	7.32		Weathered Basement
	III	3403.481				Fresh Basement
A_2	I	204.081	0.96	0.96	H	Topsoil
	II	86.319	11.8	12.8		Weathered Basement
	III	2652.3				Fresh Basement
A_3	I	299.733	0.7	0.7	H	Topsoil
	II	61.22	12.7	14.4		Weathered Basement
	III	1445.5				Fresh Basement
A_4	I	87.958	1.408	1.41	H	Topsoil
	II	30.245	7.069	8.5		Weathered Basement
	III	3367.008				Fresh Basement
A_5	I	66.061	1.357	1.36	H	Topsoil
	II	24.269	5.094	6.5		Weathered Basement
	III	2325.011				Fresh Basement

Table IV. Result and Lithology of Geoelectrical section of profile B.

S/N	Layers	Resistivity (Ωm)	Thickness (m)	Depth (m)	Curve Type	Probable Lithology
B_1	I	1329.386	4.316	4.32	H	Topsoil
	II	156.058	18.497	54.5		Weathered Basement
	III	2331.756				fresh Basement
B_2	I	339.776	0.342	0.342	A	Topsoil
	II	1150.018	7.652	8		Weathered Basement
	III	3450.039				Fresh Basement
B_3	I	260.842	2.445	2.445	A	Topsoil
	II	268.864	17.341	19.8		Weathered Basement
	III	3448.462				fresh Basement
B_4	I	25.483	0.141	0.141	A	Topsoil
	II	237.782	28.671	29.8		Weathered Basement
	III	2156.031				Fresh Basement
B_5	I	229.499	0.543	0.543	A	Topsoil
	II	333.117	65.359	65.9		Weathered Basement
	III	2,328				Fresh Basement

Table V shows the result of profile C. The thickness and resistivity of the first layer were found to range from 0.4 m to 9.9 m and 225 Ωm to 404 Ωm respectively. The resistivity values suggest a topsoil layer. The weathered layer, which is the second layer, is encountered across the profile with a range of resistivity values between $2.582 - 22.23\ \Omega m$ and thickness from $2.018 - 22.3\ m$. The resistivity value of the third layer is from $288 - 03316\ \Omega m$ with fractured basement occurrence at a thickness of 8.8445 m at VES C5. The curve types are H-type ($\rho_1 > \rho_2 < \rho_3$) except for VES C3 having A-type ($\rho_1 < \rho_2 < \rho_3$).

Table VI depicts the results of profile D. The thickness and resistivity of the first layer were found to range from 0.69 m to 1.47 m and $204 - 270\ \Omega m$ respectively. The weathered layer whichforms the second layer is encountered across the profile with a resistivity value range of 77.3 Ωm to 116.8 Ωm with a thickness value ranging from 3.48 m to 13.7 m. The third layer, which is the fresh basement has a resistivity value of 1205 Ωm to 3030 Ωm with an infinite thickness and occurrence of fractured at VES D4 resistivity ranging $69.49 - 1464.782\ \Omega m$ with a thicknessof 11.78 m and VES D5 with resistivity ranging from $67.833 - 847.012\ \Omega m$ and a thickness of $10.63\ m$. All the curve types shown in Table VI are H-types ($\rho_1 > \rho_2 < \rho_3$) except D4 having QH-type ($\rho_1 > \rho_2 > \rho_3 < \rho_4$) and D5 having Q- type ($\rho_1 > \rho_2 > \rho_3$).

The geophysics software RES2DINV was used to interpret and create inverse images of measured data of the Geoelectric/Geologic section and the results of interpretation are given in Fig. 5, 6, 7 and 8.

Table V. Result and Lithology of Geoelectrical section of profile C.

S/N	layers	Resistivity (Ωm)	Thickness (m)	Depth (m)	Curve Type	Probable Lithology
C_1	I	404.152	0.418	0.42	H	Topsoil
	II	16.982	22.26	22.7		Weathered Basement
	III	2880.27				Fresh Basement
C_2	I	379.527	0.864	0.9	H	Topsoil
	II	113.787	2.018	2.92		Weathered Basement
	III	3258.64				Fresh Basement
C_3	I	225.011	5.438	5.44	A	Topsoil
	II	638.269	4.153	9.6		Weathered Basement
	III	3316.78				Fresh Basement
C_4	I	330.603	0.864	0.9	H	Topsoil
	II	211.477	2.582	43.5		Weathered Basement
	III	2506.438				Fresh Basement
C_5	I	227.365	9.889	9.89	H	Topsoil
	II	129.758	8.8448	18.8		Weathered Basement
	III	846.208				Fractured basement

Table VI. Result and Lithology of Geoelectrical section of profile D.

S/N	layers	Resistivity (Ωm)	Thickness (m)	Depth (m)	Curve Type	Probable Lithology
D_1	I	244.595	1.467	1.47	H	Topsoil
	II	77.309	11.38	12.9		Weathered Basement
	III	3030.149				Fresh Basement
D_2	I	273.451	1.049	1.05	H	Topsoil
	II	93.466	13.691	14.8		Weathered Basement
	III	1205.351				Fresh Basement
D_3	I	270.568	1.464	1.5	H	Topsoil
	II	107.277	11.931	13.4		Weathered Basement
	III	1869.175				Fresh Basement
D_4	I	229.477	0.856	0.86	QH	Topsoil
	II	111.477	5.275	6.14		Weathered Basement
	III	69.486	11.767	17.9		Fractured basement
		1464.782				Fresh Basement
D_5	I	204.404	0.692	0.7	Q	Topsoil
	II	116.833	3.479	4.18		Weathered Basement
	III	67.833	10.63	14.81		Fractured basement
		847.012				Fractured basement

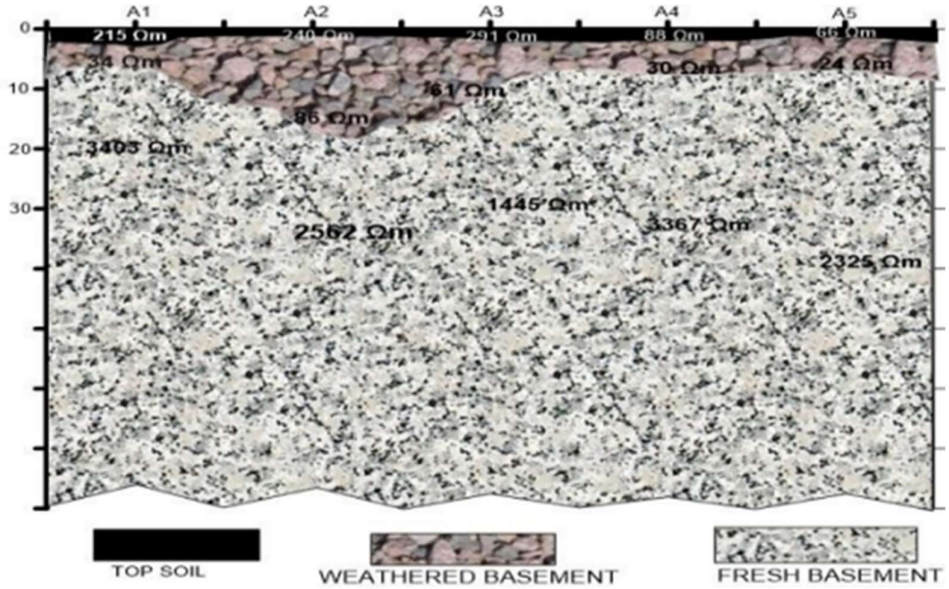

Fig. 6. Geoelectric section of profiles.

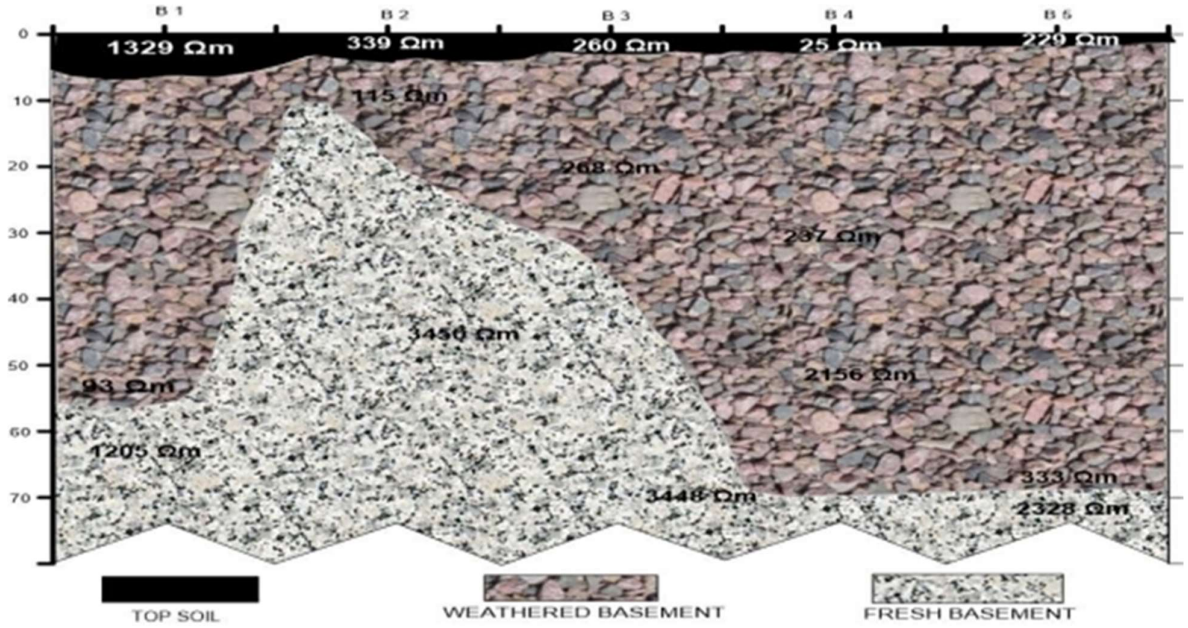

Fig. 7. Geoelectric/Geologic section of profile B.

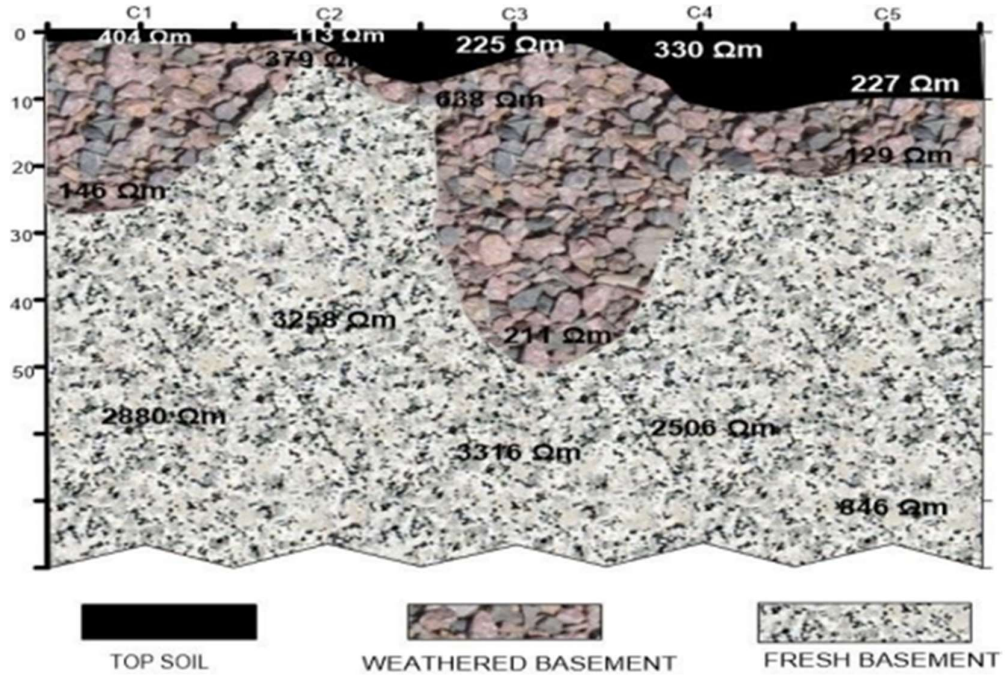

Fig. 8. Geoelectric/Geologic section for profile C.

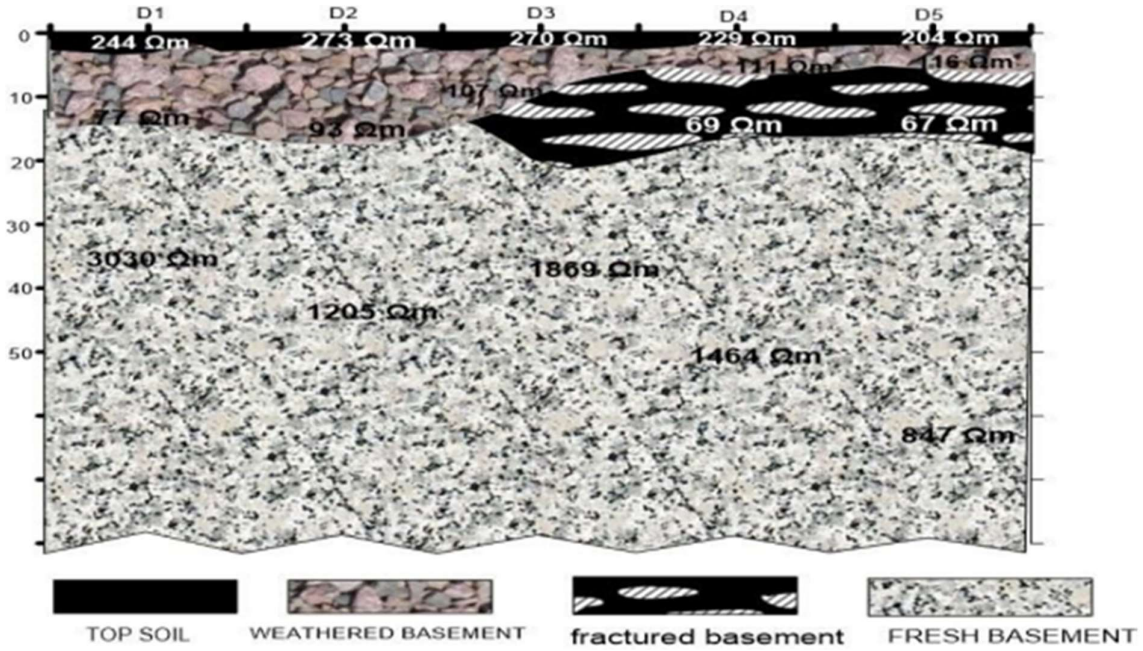

Fig. 9. Interpreted Geoelectric/Geologic section of profile D.

Fig. 6 displayed a Geoelectric/Geologic section with a total depth of 80 m. From Profile (A), five (5) Vertical Electrical Sounding (VES) were established and designated as VES (A_1-A_5). The profile described three (3) geoelectric layers which were topsoil, weathered basement and fresh basement. The top layer (soil) depicted in Fig. 6 has a depth of 2 m to the subsurface with an apparent resistivity range between $66-240\ \Omega m$. The layer (A_2) has the highest value $(240\ \Omega m)$ at a depth of 3 m while layer (A_5) has the least resistivity value (66 Ωm) at a depth of 2 m. The weathered basement has resistivity ranging from $24-161\ \Omega m$ at a depth of $5-18\ m$. The fresh basement has resistivity ranging between

1445 – 3405 Ωm at a depth between 18 – 80 m. Therefore, the region with the low resistivity value is suspected to be an aquiferous zone.

Fig. 7 displayed the geoelectric layers of profile B designated as $(B_1 - B_5)$. The profile produced topsoil, a weathered basement and fresh basemen layers. The topsoil resistivity ranges from 25.5 – 1329 Ωm with thicknesses ranging from 0.14– 4.3 m. The weathered basement has resistivity ranging from 93 – 1150 Ωm and a thickness ranging from 7.6– 68.4 m. The fresh basement has resistivity ranging from 1205 – 3448.5 Ωm.

Fig. 8 shows the geoelectric section for profile C with three interpreted subsurface layers. The thickness and resistivity of the topsoil were found to range from 0.4 – 9.9 m and 225 – 40 4 Ωm respectively. The resistivity values suggest a topsoil layer. The weathered layer which is the second layer is encountered across the profile with a range of resistivity values between $129 - 638\ \Omega m$ and thickness from $2.018 - 22.30\ m$ while the resistivity value of the fresh basement (third layer) is from $846 - 3316\ \Omega m$ with an extended thickness of $8\ m$.

Fig. 9 shows the geoelectric for profile D with three to four interpreted subsurface layers. The thickness and resistivity of the topsoil (first layer) were found to range from $0.69 - 1.47\ m$ and $204 - 270\ \Omega m$ respectively. The weathered layer which forms the second layer is encountered across the profile with a resistivity value range of $77.3 - 116.8\ \Omega m$ with thickness values ranging from $3.48 - 13.7\ m$. The third layer is the fracture zone with resistivity ranging 69 – 67 Ωm with thickness between 10.63 – 13 m. The fourth layer is the fresh basement with resistivity ranging from 847– 3030 Ωm with thickness beyond 13 m.

Table VII shows the classification system for overburden thickness protective capacity rating based on total longitudinal unit conductance values, which was used to determine the aquifer protective capacity rating.

Table VII. Overburden thickness protective capacity rating [19, 20]

Total longitudinal unit conductance	Overburden thickness protective capacity
<0.10	Poor
0.1 – 0.19	Weak
0.2 – 0.79	Moderate
0.8 – 4.9	Good
5 – 10	Very good
>10	Excellent

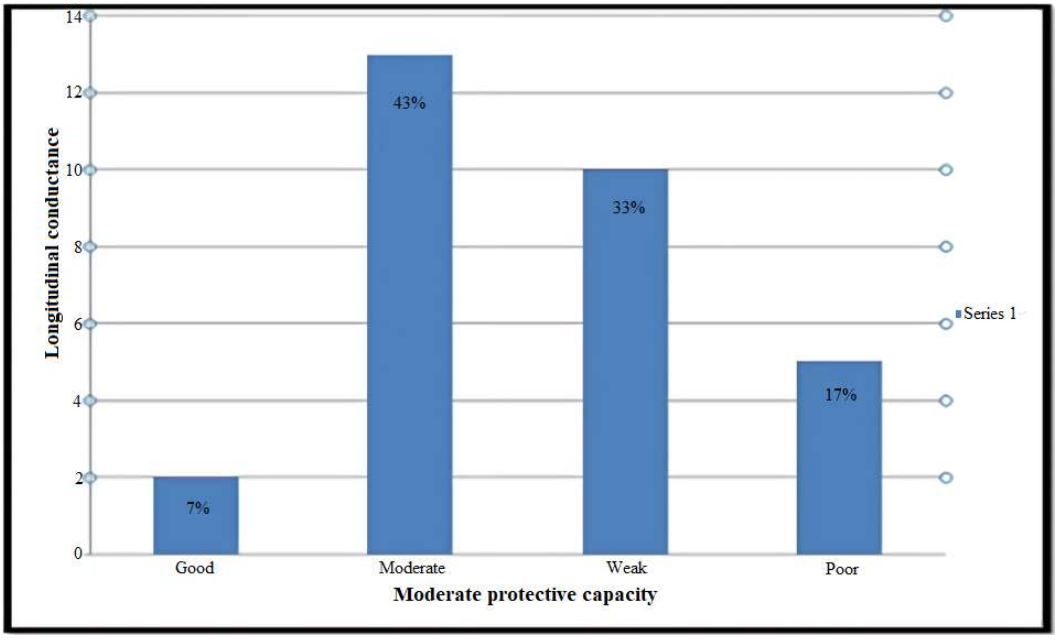

Fig. 10. A statistical representation of Aquifer protective capacity

The isoresistivity map of the topsoil resistivity produced using the Oasis Montaj application as depicted in Fig. 10 shows that 7% was good (r values between 0.8 – 4.9), 43% was moderate (r values between 0.2 -0.79), 33% was weak (r values between 0.10 - 0.19) and 17% was poor (r values < 0.10). Fig. 10 was obtained based on (13) which is embedded in the software.

The map in Fig. 11 was created by contouring the weathered basement's resistivity values at thirty (30) points along profile $A - D$. The resistivity values of the weathered basement vary between $181 - 480\ \Omega m$. Profile A and C showed relatively low resistivity values while profiles B and D showed relatively higher resistivity for the weathered basement layer.

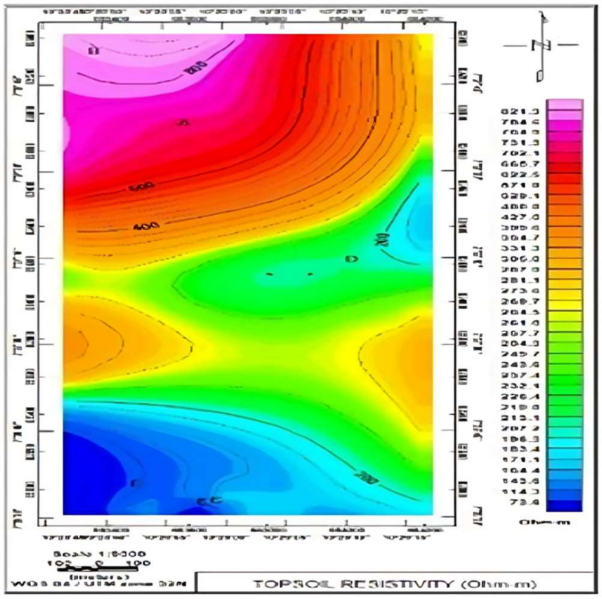

Fig. 11. Topsoil resistivity map.

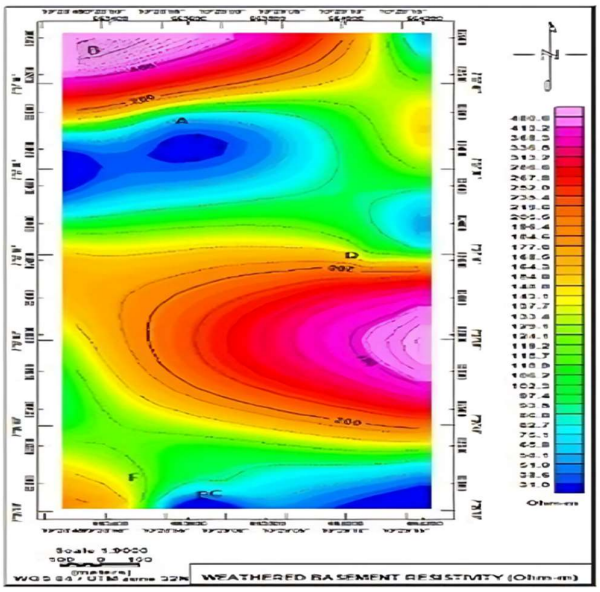

Fig. 12. Weathered basement resistivity map.

B. Fractured basement resistivity map

Fig. 13 showed the resistivity map of the fractured basement. The resistivity values of the fractured basement ranged from $1.929 - 885\ \Omega m$.

C. Fresh basement map

Fig. 14 is the fresh basement map showing relatively dominant higher resistivity trending toward the North end part of the map with values ranging from $2000 - 33000\ \Omega m$.

The Vertical Electrical Sounding performed in the study area revealed the following four Vertical Electrical Sounding curves A, H, Q and QH, and the Geoelectric/Geologic section's four geo-electric layers namely topsoil, weathered basement, fractured basement and fresh basement. The aquifer is found between the second and third layer of VES profiles A, B, C and D at depths between $0.141 - 22.7\ m$. Results from the 2D map revealed low resistivity within the weathered basement and fracture basement with resistivity values between $1.929 - 885\ \Omega m$. Both the VES and Geoelectric/ Geologic section were used to determine the depth to the groundwater, aquifer thickness, and sub-surface lithology of the study area, thus revealing its groundwater distribution.

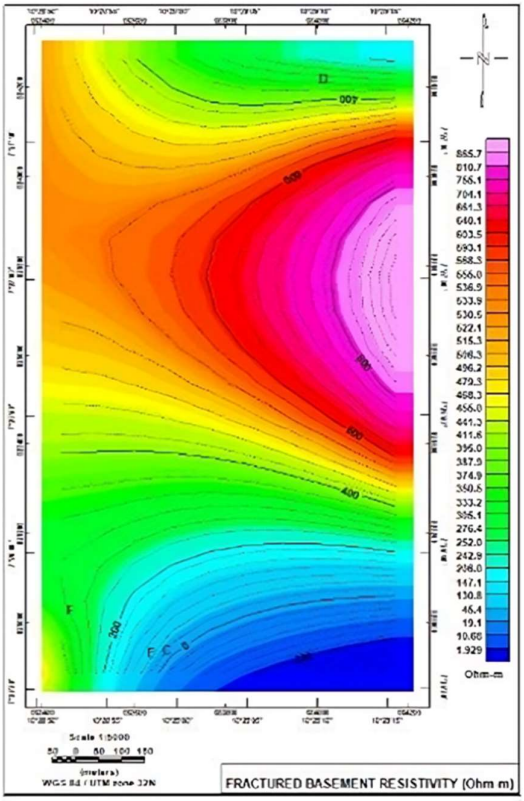

Fig. 13. Fractured basement map.

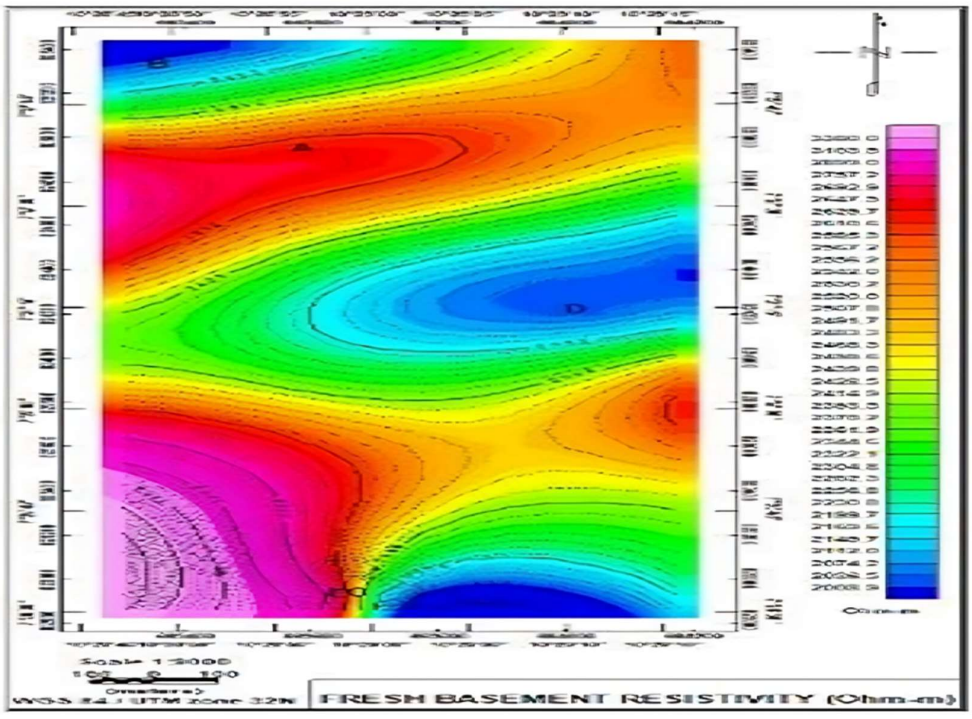

Fig. 14. Fresh basement map.

IV. CONCLUSION

The delineation of Groundwater aquifer and subsurface structures of some selected areas in Chikun Local Government Area of Kaduna State was carried out using Vertical Electrical Sounding (VES) method, with results revealing that the aquifers were at the depths $7.3, 0.141 - 22.7\ m$, and $14\ m$ for VES A, B, C and D respectively. The results of the geoelectrical section of the study area revealed similar results to that of VES. The depth to the aquifer across the study area lies between $0.141 - 22.7\ m$, with the geologic layer of the aquiferous zone characterized by fractures and porosity aiding groundwater permeability and storage.

References

[1] S. A. S. Araffa. Delineation of groundwater aquifer and subsurface structures on North Cairo, Egypt, using integrated interpretation of magnetic, gravity, geoelectrical and geochemical data. *Geophy. J. Int.*, vol. 192, no. 1, pp. 94–112, 2013. https://doi.org/10.1093/gji/ggs008

[2] W. Shafqullah, S. Hakim and M. Hideki. "Groundwater aquifer detection using the electrical resistivity method at Ito Campus, Kyushu University". Geosci. Lett., vol. 8, no. 15, *2021*. https://doi.org/10.1186/s40562-021-00188-6

[3] F. P. M. Bierkens1 and Y. Wada. "Non-renewable groundwater use and groundwater depletion". Env. Res. Lett., vol. 14, 063002, 2019. https://iopscience.iop.org/article/10.1088/1748-9326/ab1a5f

[4] S. Siebert, M. Kummu, M. Porkka, P. Döll, N. Ramankutty and B.R. Scanlon, "A global data set of the extent of irrigated land from 1900 to 2005" Hydro. Earth Syst. Sci., vol. 19, pp. 1521–45, 2015.

[5] A. Y. Hoekstra and A. K. Chapagain. "Water footprints of nations: water use by people as a function of their consumption pattern". Wat. Res. Mgt., vol. 21, pp. 35–48, 2007.

[6] A. M. MacDonald "Groundwater quality and depletion in the Indo-Gangetic Basin mapped from in situ observations" Nat. Geosci., vol. 9, pp. 762–6, 2016.

[7] T. Gleeson, Y. Wada, M. F. P. Bierkens and L. P. H. van Beek, "Water balance of global aquifers revealed by groundwater footprint, Nat., vol. 488, pp. 197–200, 2012.

[8] O. O. Isaac., C. A. Jonah and O . A . Joel, " Assessment of Aquifer Characteristics in Relation to Rural Water Supply in Part of Northern Nigeria*". Res., vol. 2, no. 3, pp. 22-27, 2010..*

[9] M. H. Loke, T. Dahlin, D. F. Rucker. "Recent developments of the direct-current geoelectrical imaging method". Geophy., vol. 95, pp. 135–156, 2014.

[10] G. El-Qady, K. Ushijima. "Inversion of DC resistivity data using neural networks". Geophy. Prosp., vol. 49, pp. 417–430, 2011.

[11] N. Greggio, B. M. S. Giambastiani, E. Balugani, C. Amaini and M. Antonellini. "High-resolution electrical resistivity tomography (ERT) to characterize the spatial extension of freshwater lenses in a salinized coastal aquifer". Water, vol. 10, no. 8, pp. 1067. 2018. https://doi.org/10.3390/w10081067

[12] A. Sendros, M. Himi, R. Lovera, L. Rivero, R. Garcia-Artigas, A. Urruela and A. Casas. "Electrical resistivity tomography monitoring of two managed aquifer recharge ponds in the alluvial aquifer of the Llobregat river (Barcelona, Spain)". Near Surf. Geophy., vol. 18, no. 4, pp. 353–368, 2020. https://doi.org/10.1002/nsg. 12113

[13] H. O. Aboh. "Assessment of the aquifers in some selected villages in Chikun local government area, Kaduna state, Nigerian. Sci. World J., vol 4, no 2, pp. 37-42, 2009.

[14] M. John. "Field Geophysics" 3rd Ed. Univ. Coll. London: John Wiley and Sons Ltd. 2003.

[15] C. G. Afuwai. "Understanding the basics of electrical resistivity Geophysical survey, federal university Dutsin-ma Nigeria". Lambert Academic Publishing. 2013.

[16] C. E. Osele, A. G. Onwuemesi, E. K. Anakwuba, A. I. Chinwuko. "Application of vertical electrical sounding (VES) for groundwater exploration in Onitsha and environs, Nigeria". Int. J. of Adv. Geosci., vol. 4, no. 1, pp. 1-7, 2016.

[17] A. A. Theophilus. Margaret K. A. Margaret, A. Lukman, A. P. Sunmonu. Aizebeokhai, 1. K. Aizebeokhaid, 1. Oyeyemi and O. A. Felicia. "Groundwater exploration in Aaba Residential area of Akure Nigeria". Frontiers in Earth Sci., 2018.

[18] M. I. Oladapo and O. J. Akintorinwa. "Hydrogeophysical study of Ogbese southwestern Nigeria". Global J. of Pure and App. Sci., vol. 13, no. 1, pp. 55-61, 2007. https://doi.org/10.4314/gjpas.v13i1.16726

[19] A. E. Adeniji, O. V. Omonana, D. N. Obiora and J. U. Chukudebelu. "Evaluation of soil corrosivity and Aquifer protective capacity using Geo-Electrical Investigation in Bwari basement area, Abuja". J. of the Earth Syst. Sci., vol. 123, no. 3, pp. 491-502, 2014.

[20] M. Oladapo, M. Mohammed, O. Adeoye and B. Adetola. "Geoelectrical investigation of the Ondo state housing corporation Estate Ijapo Akure, Southernwestern". Nig. J. on Min. & Geol., vol. 40, pp. 41-48, 2004.